JOURNAL OF PHYSICAL ORGANIC CHEMISTRY
J. Phys. Org. Chem. 2007; **20:** 469–483
Published online 29 April 2007 in Wiley InterScience
(www.interscience.wiley.com) DOI: 10.1002/poc.1181

Investigation of cation complexation behavior of azacrown ether substituted benzochromene

O. A. Fedorova,[1]* F. Maurel,[2] A. V. Chebun'kova,[1] Yu. P. Strokach,[1] T. M. Valova,[1] L. G. Kuzmina,[3] J. A. K. Howard,[4] M. Wenzel,[5] K. Gloe,[5] V. Lokshin[6] and A. Samat[6]

[1]Photochemistry Center of RAS, Novatorov str. 7a, 119421 Moscow, Russia
[2]ITODYS, Université Paris 7, CNRS (ESA 7086), 1 Rue Guy de la Brosse, 75005 Paris, France
[3]Institute of General and Inorganic Chemistry, RAS, Leninskii Pr. 31, 117907 Moscow Russia
[4]Department of Chemistry, University of Durham, South Road, Durham, DH1 3LE, UK
[5]Technical University Dresden, Department of Chemistry, Laboratory of Coordination Chemistry, Bergstr. 66, 01062 Dresden, Germany
[6]Faculte des Sciences de Luminy, Universite de la Mediterranee, UMR 6114 CNRS, 13288 Marseille, France

Received 21 December 2006; revised 21 February 2007; accepted 5 March 2007

ABSTRACT: The study of the complex formation of 3,3-diphenyl-3*H*-benzo[f]chromenes containing aza-18-crown-6-ether, diaza-18-crown-6-ether or morpholine units with alkali, alkaline earth, heavy and transition metal cations in acetonitrile is reported. The spectroscopic and kinetic behavior of the photomerocyanine isomers of these chromenes is strongly affected by complexation with a metal cation. In order to interpret some of experimental data, an *ab initio* theoretical analysis of photochromic-crown ether and its cation complexes was conducted. The different site of coordination of mono- and divalent cations to determine the minimum-energy structure of benzochromene complexes in gas phase as well as in acetonitrile as solvent was explored. The coordination of both carbonyl oxygen and crown-ether macrocyle with divalent cations in carbonyl-capped structure is found to be the most stable isomer in gas as well as in condensed media. The crown-containing benzochromenes were studied in liquid-liquid extraction experiments toward there capacity to transfer metallic salts from water into an organic phase.The high selectivity to extraction of Ag^+ was found. Copyright © 2007 John Wiley & Sons, Ltd.
Supplementary electronic material for this paper is available in Wiley InterScience at http://www.interscience.wiley.com/jpages/0894-3230/suppmat

KEYWORDS: aza-18-crown-6-ether; 3,3-diphenyl-3H-benzo[f]chromene; complex formation; photochromic behavior; anion-'capped' complex

INTRODUCTION

Photochromic compounds have received great interest in the last years due to their application such as ophthalmic lenses, transparencies, plastic films, promising materials for the information imaging and storage, etc.[1–5] The development of these photochromic systems is aimed at the improved photo stability, to obtain higher sensitivity, a wide choice of operating wavelengths and amplification capability.[6–9] Incorporation of a crown ether moiety, which is able to bind metal ions into the molecule skeleton can be explored to tune the photochromic properties by using a complexation process.[10–14] The approach has been found to be effective for different kinds of photochromic compounds.[15,16] The synthesis and investigation of the benzochromenes containing ionophoric groups have not been enough studied, there are only few papers on this topic.[17–19]

In the present paper the series of the benzochromenes **1a-c** containing morpholine, aza- and diaza-18-crown-6 ethers have been prepared and studied. The synthesis and first results toward the photochromic properties of the free compound **1b** and its complex with Na^+ cation were described in ref.[19] The ability of aza – and diazacrown ethers to form complexes with different kinds of metal cations is well-known.[20] We investigated the complex formation with alkali, alkaline earth, heavy and transition metal cations and analyzed what structure of the complex forms for each type of metal cations and how the formed complex influences the spectral and photochromic properties of benzochromenes **1a-c**. The structural variation of the benzochromene plays an important role in the understanding of the observed phenomena. The results presented in this contribution substantially extend

**Correspondence to:* O. A. Fedorova, Center of Photochemistry at the Joint N.N.Semenov Institute of Chemical Physics of the Russian Academy of Sciences, ul.Novatorov 7a, 117421 Moscow, Russia.
E-mail: fedorova@photonics.ru

the knowledge and understanding of possibility to apply the ionophoric fragments in this type of benzochromene for the modification of the spectral and photochromic characteristics.

RESULTS AND DISCUSSION

Synthesis

The compounds were synthesised according to the three-step procedure[19] represented in Scheme 1. The structures attributed to **1a-c** were confirmed by ^{1}H NMR spectroscopy data, mass-spectrometry and elemental analysis (experimental data were presented in short report[21]).

Crystal structure of 1a

The molecule structure of **1a** and atom numbering scheme are shown in Fig. 1. Bond lengths and separated bond angles are given in Supplementary materials (in Tables S1, S2).

All geometric parameters of molecule **1a** correspond to standard values. The naphthalene fragment has commonly observed bond length distributions; in each of six-membered rings two bonds [C(4)—C(13) 1.388(3), C(11)—C(12) 1.372(2), C(6)—C(7) 1.370(3) and C(8)—C(9) 1.358(4) Å] are somewhat shortened compared to others varying from 1.394(4) to 1.430(3) Å.

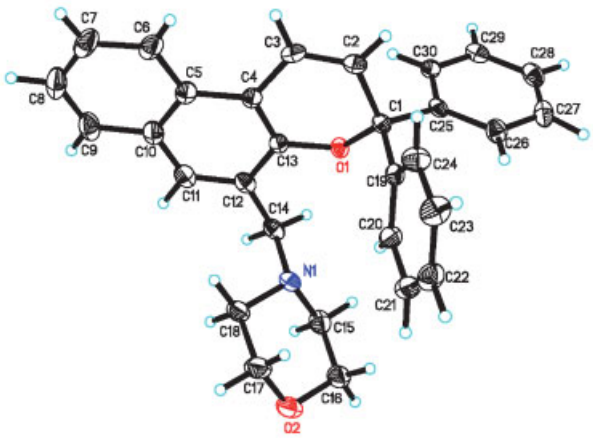

Figure 1. Structure of molecule **1a**. Atomic thermal ellipsoids are drown on 50% probability level

The ethylene bond C(2)—C(3) is essentially shortened [1.324(2) Å]. The oxygen-containing six-membered ring has a sofa conformation. Atoms C(2)—C(3)—C(4)—C(13)—O(1) lie in the same plane, whereas C(1) deviates by 0.393 Å from this plane. The corresponding bent angle composes 27.2°. The C(19)...C(24) benzene ring has a pseudo-axial orientation, whereas the C(25)...C(30) ring, a pseudo-equatorial orientation.

The morpholine ring adopts a chair conformation, with the bent angles equal to 52.7 and 51.4° for the N and O angles, respectively.

The structure of **1a** does not contain an 'active' proton and its crystal packing has no specific weak interactions.

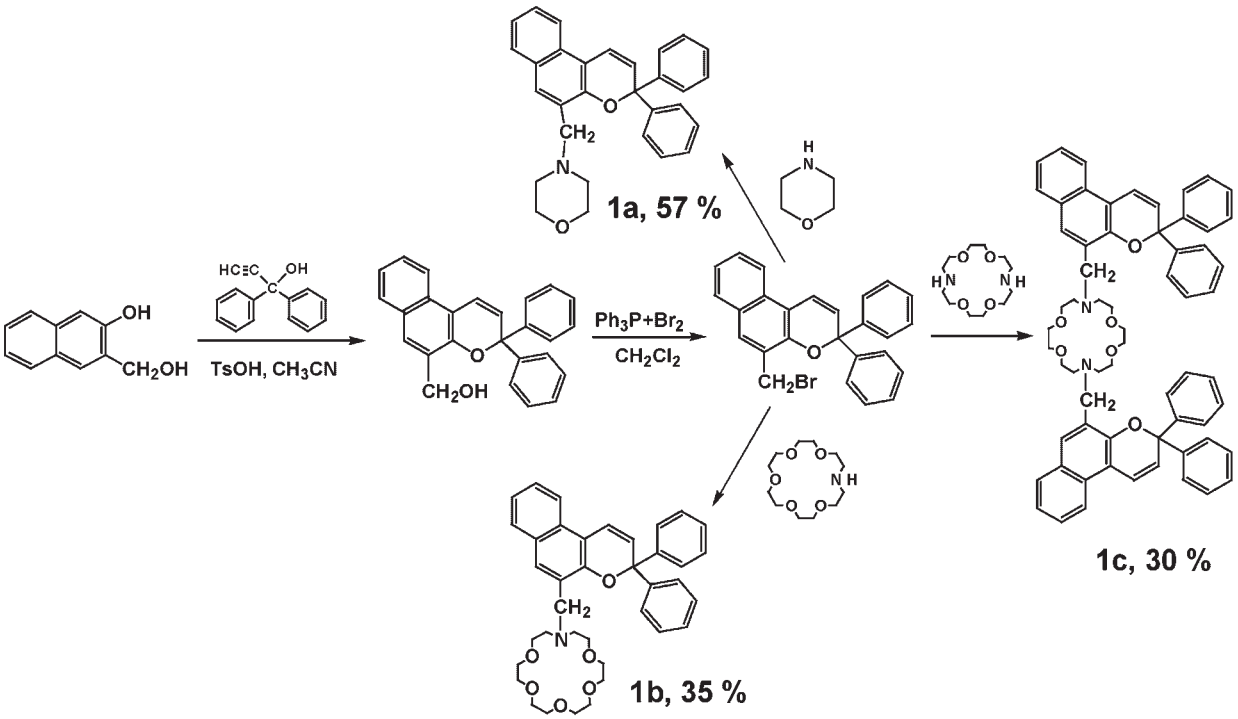

Scheme 1

DOI: 10.1002/poc

All the interatomic contacts correspond to the van der Waals interactions.

Complex formation and phototransformation

Compounds **1a-c** in MeCN exhibited very similar UV/Vis absorption spectra. The addition of equimolar amount of Mg^{+2}, Sr^{+2}, Ba^{+2}, Ag^{+}, Cd^{+2}, Pb^{+2} to a solution of **1b** leads to the small bathochromic shift up to 5–10 nm of the long wavelength band, indicating that metal cation is bound by the macrocyclic unit of **1b,c** (Scheme 2). In contrast, the absorption spectrum of **1a** was affected only at a high metal cation concentration ($0.1\ mol \cdot dm^{-3}$) (the effect of large amount of metal cations on spectral characteristics are shown in Table 1).

UV irradiation of **1a-c** in MeCN results in the appearance of a broad absorption band in the visible region, which was assigned to the merocyanine isomer (Scheme 3). The dark ring-closure reaction for merocyanine isomers PM**1a-c** occurs with a rate constant $k_{MF\text{-}CF}$ of about 0.05, 0.094, $0.08\ s^{-1}$ respectively and resulted in the initial chromene. The presence of the metal cation in the solution of photomerocyanine form leads to a significant change in the dark lifetime of PM**1a-c** and causes the strong shifts in their absorption spectra, indicating that these compounds are able to bind metal cations (Fig. 2, Table 1).

The addition of the alkali, alkaline earth metal cations does not affect the position of the long wavelength maximum of PM**1a**, except Mg^{2+}. The shift of the band to the long wavelength region up to 40 nm was found in the last case. The similar shifts were found when Ag^{+}, Cd^{+2}, Pb^{+2} were added to the solution of PM**1a**. In the presence of alkali, alkaline earth metal cations, mentioned metal cations Ag^{+} and Cd^{+2} the constant of thermal relaxation of the PM**1a** decreases. The complex formation of the PM**1a** can occur through the formation of the coordination bond between metal cations and carbonyl oxygen atom. As we showed early, this type of the coordination is very weak.[22]

In the merocyanine form of benzochromenes **1b,c** there are two places for the coordination of metal cations: crown ether fragment and carbonyl oxygen atom.

The addition of all listed metal cations to the solution of PM**1b,c** leads to the substantial bathochromic shift (20–80 nm) of the long wavelength band. The analysis of the influence of metal cations on the kinetic of thermal relaxation of **1b,c** allows us to divide the studied cations into 3 groups. In the presence of small monovalent cations (Li^{+}, Na^{+}) rate constant $k_{MF\text{-}CF}$ of the dark ring-closure reaction for merocyanine isomer decreases. So as the size of the cation is too small in comparison with the size of aza-18-crown-6 ether cavity, the formation of an inclusion complex with crown ether fragment is not possible. It is obvious, that the formation of the coordination bond between Li^{+} or Na^{+} and carbonyl oxygen atom similar to **1a** can be anticipated. The coordination causes the stabilisation of the open form (Table 1, Scheme 5).

Table 1. Absorption maximum of the initial closed (λ_{CF},nm) and photoinduced merocyanine (λ_{MF},nm) forms, and constant of the thermal relaxation of the colored form ($k_{MF\text{-}CF}$,s^{-1}) of **1a-c** and its complexes with different metal cations; $C_{Lig} = 2 \times 10^{-4}$ mol/l, $C_{Lig}/C_{Met} = 1/100$ in MeCN, L = 1 cm; irradiation with light at $\lambda = 365$ nm

Chromene	Metal cation	λ_{CF}, nm	λ_{MF}, nm	$k_{MF\text{-}CF}$,s^{-1}
1a		355	422	0.5
	Li^{+}	355	420	0.17
	Na^{+}	355	420	0.13
	Mg^{2+}	360	460	0.024
	Sr^{2+}	355	420	0.16
	Ba^{2+}	355	420	0.15
	Ag^{+}	365	462	0.39
	Cd^{2+}	360	467	0.30
	Pb^{2+}	365	465	0.67
1b		355	420	0.094
	Li^{+}	360	450	0.008
	Na^{+}	360	440	0.013
	Mg^{2+}	365	470	0.16
	Sr^{2+}	360	470	0.0021
	Ba^{2+}	360	460	0.0057
	Ag^{+}	365	460	0.26
	Cd^{2+}	365	495	0.0042
	Pb^{2+}	360	500	0.005
1c		360	405	0.08
	Li^{+}	360	440	0.042
	Na^{+}	360	430	0.015
	Mg^{2+}	360	470	0.13
	Sr^{2+}	360	465	0.011
	Ba^{2+}	360	450	0.0005
	Ag^{+}	355	460	0.13
	Cd^{2+}	360	490	—
	Pb^{2+}	360	490	0.006

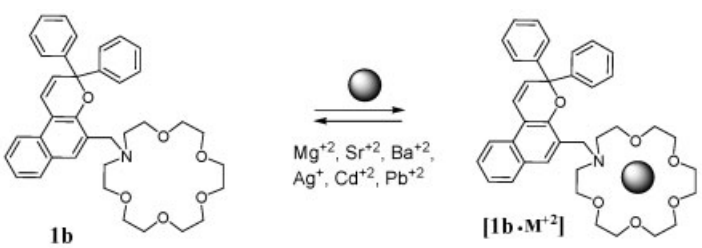

Scheme 2

DOI: 10.1002/poc

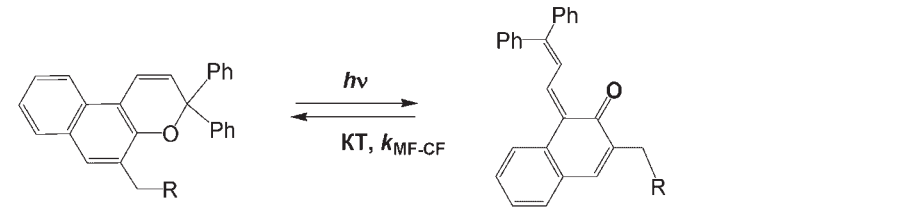

closed form (CF) **1a-c** photoinduced merocyanine form PM**1a-c**

Scheme 3

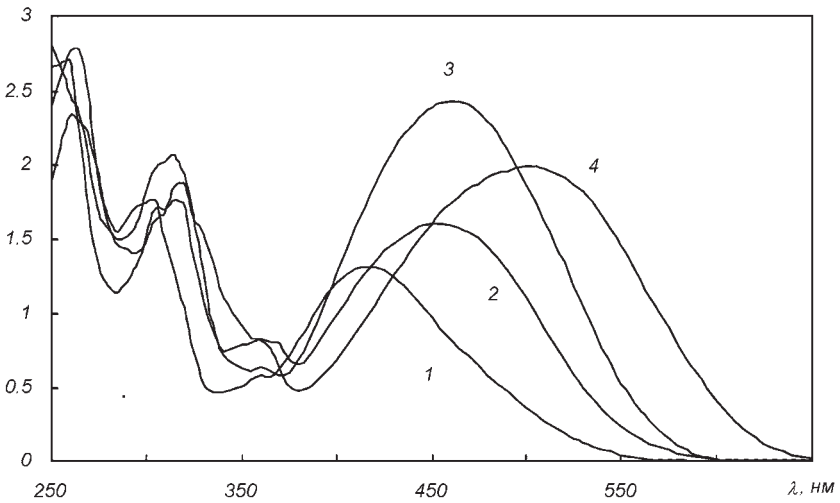

Figure 2. UV/Vis spectrum of PM**1b** in acetonitrile: (1) -free PM**1b**; (2) -in the presence of $Mg(ClO_4)_2$; (3) -in the presence of $Ba(ClO_4)_2$; (4) -in the presence of $Pb(ClO_4)_2$, prepared by irradiation of solution with light at 365 nm; $[C_L] = [C_M^{2+}] = 2 \cdot 10^{-4}$ mol/L

The metal cations Mg^{+2} and Ag^{+} belong to the second group. They decrease the stability of the open form (Table S1 of the supplementary materials). For these cations the preferred place for binding in **1b,c** is the crown ether cavity (Scheme 6). The presence of metal cation into the composition of merocyanine open form causes the polarisation of open form. The ring-closure reaction should be accelerated in polar molecule.

The formation of a 1:1 complex between open form of **1b,c** and Ba^{2+}, Cd^{2+} and Pb^{2+} is accompanied by a large bathochromic effect and the substantial decrease of the rate constant for dark ring-closure reaction. To explain the results we suggested the formation of the carbonyl-' capped' complex of metal cation located in crown ether cavity with carbonyl oxygen atom (Scheme 6). Only the participation of both coordination centers gives substantial changes in the UV spectra as well as remarkable stabilisation of open merocyanine form. The formation of the carbonyl-'capped' complex was found early for the crown-containing spironaphthoxazines.[11,14,23]

To analyse the formation of 'carbonyl' capped complexes the kinetics of ring-closed reactions of this complexes were carefully studied at equimolar ration between ligand and metal cations (Table 2). In case of **1b,** the effect depends on the nature of metal cations; it is larger for Pb^{2+} than for Ba^{2+}. We found that in the presence of Pb^{2+} PM**1b** and PM**1c** exhibit similar values for $k_{MF-CF} \cdot s^{-1}$ (0.00035 and 0.00054, see Table 2). Whereas, the open form of Ba^{2+} complex of PM**1c** is much more stable than those of PM**1b** (0.0016 and

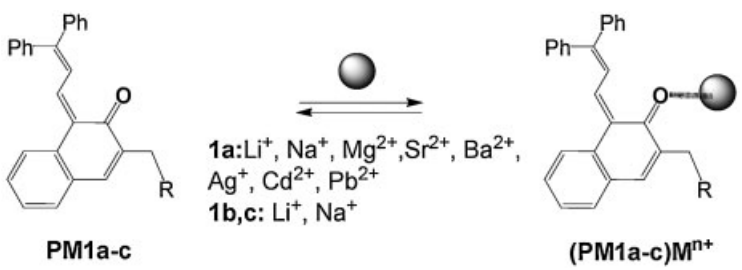

PM1a-c **(PM1a-c)M^{n+}**

Scheme 4

DOI: 10.1002/poc

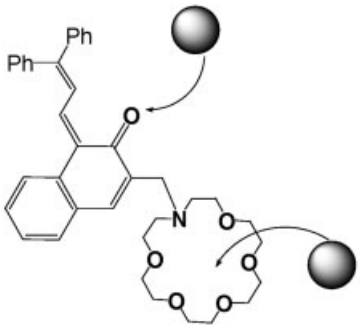

Scheme 5

0.00035 accordingly, see Table 2). We believe that in the complex of PM**1c** with Ba^{2+} the carbonyl atoms of both photomerocyanine units participate in the formation of carbonyl-'capped' complex, whereas, in the carbonyl-'capped' complex of PM**1b** Ba^{2+} forms only one coordination carbonyl-metal bond (Schemes 6 or 7). In contrast, for the complexes of PM**1b** and PM**1c** with Pb^{2+} the magnitudes of $k_{MF\text{-}MF}s^{-1}$ are similar to each other, what suggest the participation of only one photomerocyanine unit of PM**1c** in the formation of carbonyl-'capped' complex with Pb^{2+} (Scheme 7).

Molecular orbital calculations

To achieve a fundamental understanding of the interaction between the photochromic component and cationic guest, we have undertaken an *ab initio* theoretical analysis of photochromic crown ether and its cation complexes. The main goals of the theoretical study are (i) to predict the site of coordination of the cations in the merocyanine isomer of **1a** and **1b** and calculate the binding energies; (ii) to determine the influence of metal cations on the electronic and optical properties of the photomerocyanine form. The calculated bond lengths (in Å) for TC isomer of PM**1a,** PM**1b** and its metal complexes, relative energies (in kcal/mol) of the low-energy conformational isomers of PM**1a,b**-M^+ and PM**1a,b**-M^{2+} complexes at different levels of theory (A = H/6-31G, B = B3LYP/6-31G//HF/6-31G and C = B3LYP/6-31G//HF/6-31G in acetonitrile) presented in Tables S1–S5 (in Supplementary materials).

Table 2. Effect of the Mg^{2+}, Ba^{2+} and Pb^{2+} presence on the rate constant $k_{MF\text{-}CF}/s^{-1}$ of dark ring-closure reaction, $C_{Lig} = 2 \times 10^{-4}$ mol/l, $C_{Lig}/C_{Met} = 1/1$ in MeCN, L = 1 cm; irradiation with light at $\lambda = 365$ nm

		Mg^{2+}	Ba^{2+}	Pb^{2+}
1a	0.5	0.44	0.18	0.12
1b	0.094	0.49	0.0016	0.00035
1c	0.08	0.19	0.00034	0.00054

Energies and molecular structures. It is well known that opened isomer of benzochromene can exist as *trans-cis* (TC) or *trans-trans* (TT) isomers.[24] It was proved experimentally[24] and by calculations[18] that TC isomer was the most stable isomer for the unsubstituted benzochromene, that is 3,3-diphenyl-3*H*-benzo[f]chromene. In order to confirm that this result is general in this series we performed geometry optimisation of both

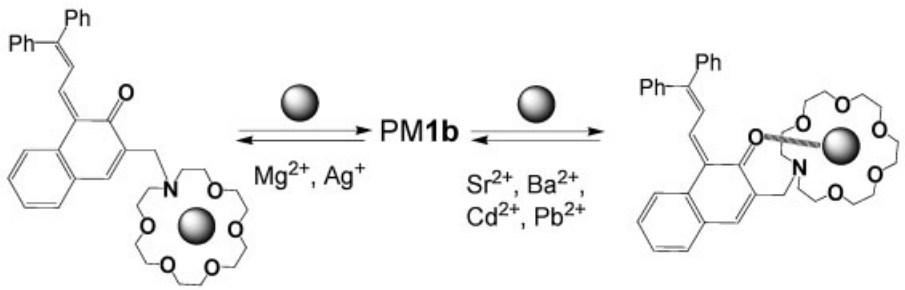

Scheme 6

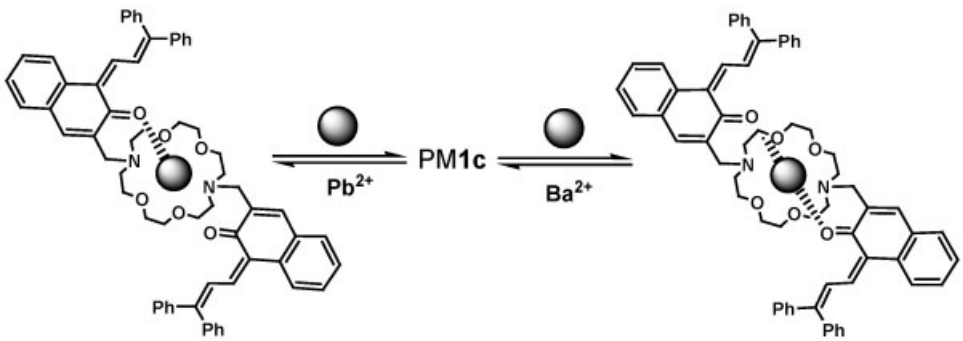

Scheme 7

DOI: 10.1002/poc

TC and TT isomer of PM**1a** and PM**1b**. Calculations indicate that TC isomer is most stable than TT by 3.4 and 1.4 kcal · mol^{-1} for PM**1a** and PM**1b** compounds, respectively (B3LYP/6-31G//HF/6-31G). On the basis of this result and for the sake of simplicity, all calculations were restricted to the TC isomer in the following although it cannot be excluded that both isomers can be present at room temperature when complexation with cation occurs.

Uncomplexed TC isomers of PM1a and PM1b.

The optimised geometry of the TC isomers of PM**1a** and PM**1b** are displayed in Fig. 3. Two minima conformations were obtained for the morpholine group: the chair like, PM**1a$_c$**, is found more stable than the twisted boat, PM**1a$_b$**, conformation by 7.9 kcal/mol (B3LYP/6-31G//HF/6-31G calculations). Although this calculation was performed on the merocyanine form, it can be anticipated that similar preference for chair like conformation should be obtained in the closed form which is consistent with X-ray crystallographic geometric structure of **1a** shown in Fig. 1. However, both conformations of the morpholine group were considered in the following to study the ability of **1a** merocyanine to bind a cation since boat like conformation allows the coordination of both nitrogen and oxygen atoms by the cation.

Previous studies of 18-crown-6-ether showed that two isomers among the many low-energy conformations can be considered at room temperature: the C_i symmetry isomer and the D_{3d} isomer (see Fig. 4). It is well established that the C_i isomer is the global minimum in the gas phase whereas D_{3d} isomer is most stable in polar solvents. This result was in agreement with our calculations in gas phase (the C_i isomer is found more stable than D_{3d} by 10.4 kcal · mol^{-1} at B3LYP/6-31G//HF/6-31G level of calculation) but only partially confirm in condensed medium since PCM model of solvation is able to obtain a valid approximation of solvent effects as long as no specific interactions (such as hydrogen bonds) between solute and solvent molecules occurs. Indeed, the free energy of solvation in acetonitrile is found +0.34 and −4.43 kcal · mol^{-1} for C_i and D_{3d}, respectively. Moreover, the D_{3d} isomer has a cavity most suitable for interactions with cationic guest. Substitution of 18-crown-6-ether by PM**1b** reduces the symmetry from C_i to C_1 and produces three isomers by substituting the endocyclic heteroatoms, i and ii and the exocyclic iii heteroatom by the nitrogen atom (see Fig. 4). Substitution of D_{3d} isomer of 18-crown-6-ether by PM**1b** reduces symmetry of the parent macrocycle to C_1. Structures of PM**1b**-D_{3d}, PM**1b**-C_i, PM**1b**-C_{ii} and PM**1b**-C_{iii} presented in Fig. 3 illustrate the respective optimised

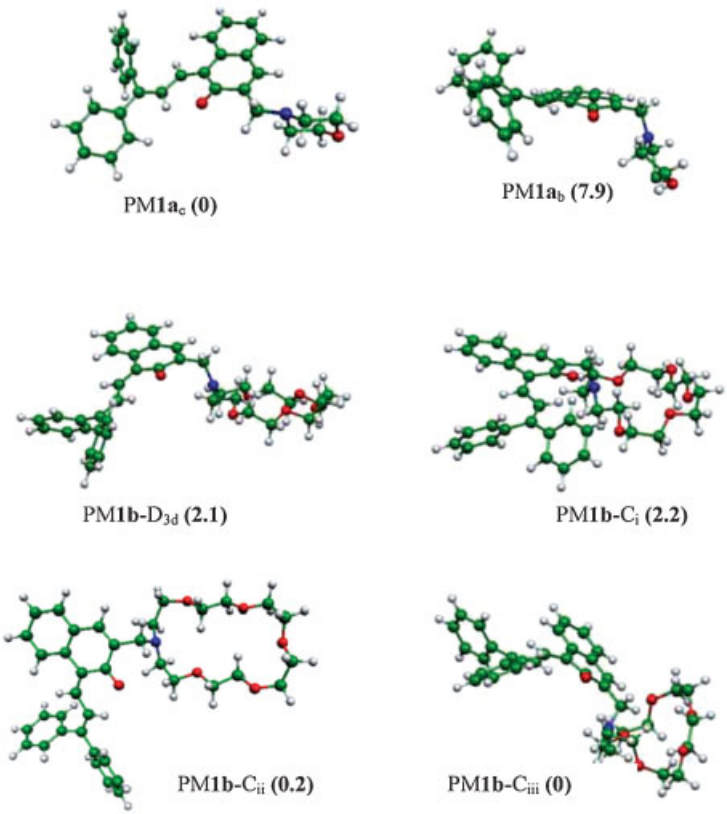

Figure 3. Ab initio optimised geometry for various conformation structures of the TC merocyanine of benzochromens **1a** and **1b**. The relative energies given in bracket (in kcal · mol^{-1}) are calculated at B3LYP/6-31G//HF/6-31G level of levels

DOI: 10.1002/poc

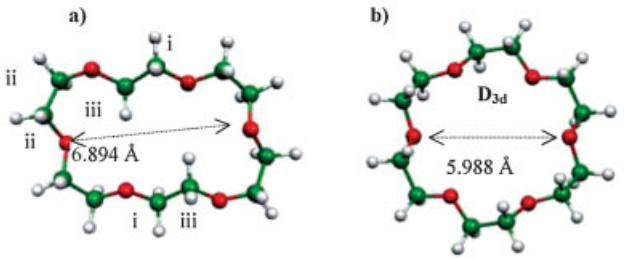

Figure 4. C_i **a)** and D_{3d} **b)** symmetry isomers of 18-crown-6-ether

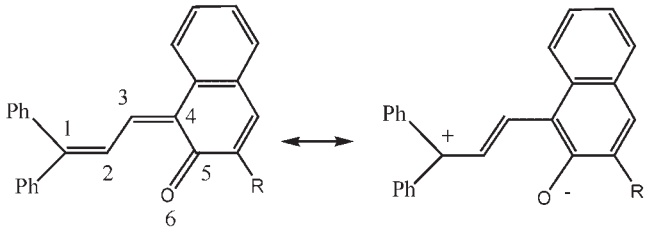

Scheme 8

geometries. Fig. 3 reveals that the PM**1b**-C_{iii} is the most stable isomer. In this isomer, the aromatic benzochromene is found located just above the macrocyle in a conformation which prevents a good interaction with cationic guest. Therefore, although the PM**1b**-D_{3d} conformational isomer is not the most stable in gas phase, we consider for the study of the PM**1b** complexes only the D_{3d} conformation of the macrocyle since the shape of the cavity allows a better interaction with cations. (see Figures 5 and 6)

The geometry of the TC merocyanine isomer can be characterised by analysing the extent of bond length alternation (BLA)[18] in the conjugated bridge connecting the donor C_1 carbon and the acceptor carbonyl groups (C_5-O_6), which reflects the relative weights of the neutral polyenic and zwitterionic structures in the valence bond (VB) resonance hybrid (Scheme 8). The BLA parameter is defined as the difference between the average length of the 'single' bonds and that of the 'double' bonds. The 'single' and 'double' bonds were identified by reference to the neutral VB structures, so high positive (negative) value of the BLA parameter indicates predominance of the neutral (zwitterionic) mesomeric structure. A vanishing BLA parameter, on the other hand, shows a cyanine-like structure characterised by similar weights of the two forms.

On this basis, the calculation results (given in Tables S5, S6 of Supplementary materials) pointed out that TC isomer of PM**1a** and PM**1b** adopts a neutral rather than zwiterrionic form in the ground state. The BLA value is found in the range between 0.230 Å and 0.238 Å suggesting that the morpholine and crown ether substituents have got a little influence on the geometric and electronic structures of the conjugated bridge. A direct consequence of this result is that the free TC isomer of PM**1a** and PM**1b** should have similar maximum absorption properties (*vide supra*) as indicated from experiment findings.

TC isomer of PM1a and PM1b complexes with Li^+, Na^+, Mg^{2+}, Ba^{2+} and Pb^{2+}. The mono- or divalent cation can coordinate with carbonyl oxygen of the merocyanine form (complexes are named PM**1a$_c$**-O or PM**1a$_b$**-O) or with morpholine substituent through the participation of oxygen and nitrogen atoms (structures PM**1a$_c$**-Mor and PM**1a$_b$**-Mor). A third type of

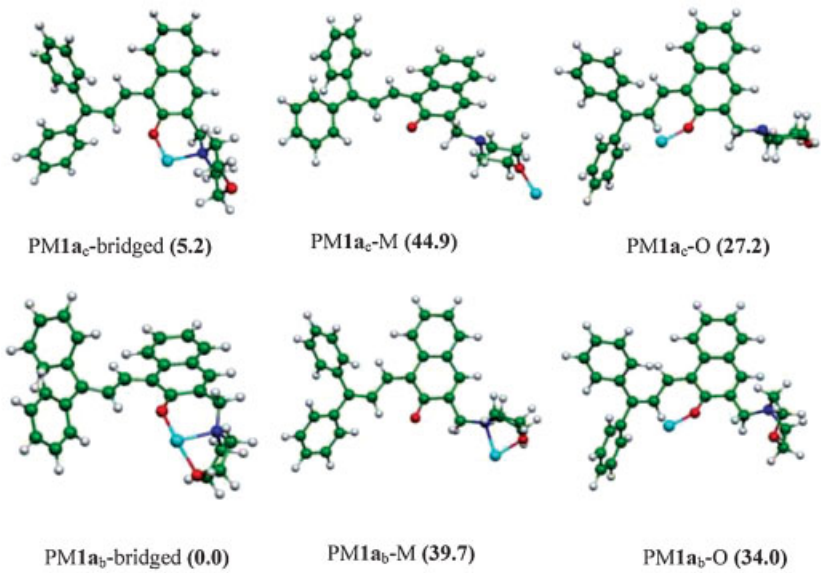

Figure 5. Ab initio optimised geometry of the various possible structures PM**1a** complexes of Li^+. The relative energies given in bracket (in kcal · mol^{-1}) are calculated with B3LYP/6-31G//HF/6-31G levels

DOI: 10.1002/poc

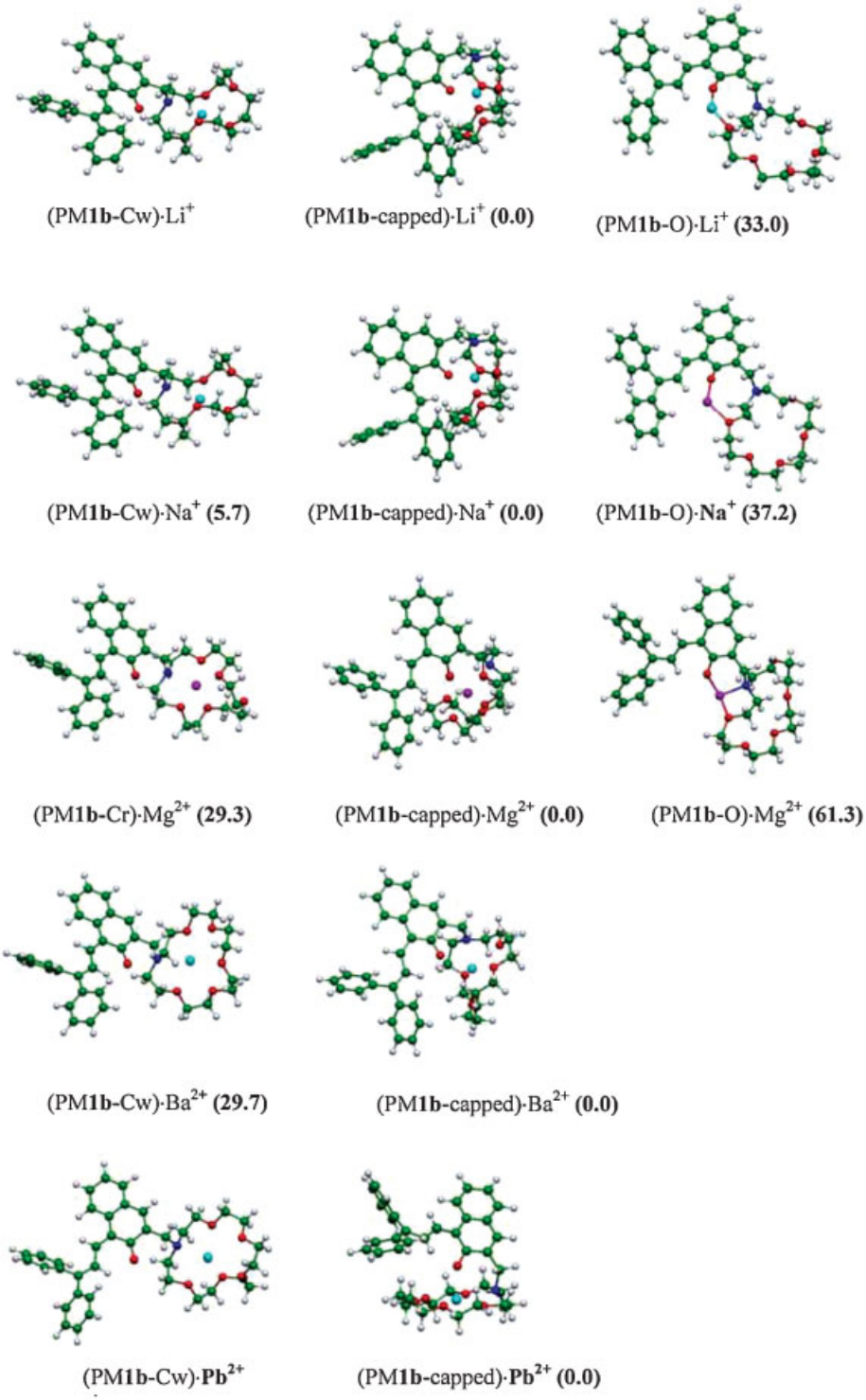

Figure 6. Ab initio optimised geometries of the PM**1b** complexes with Li^+, Na^+, Mg^{2+}, Ba^{2+} and Pb^{2+}. The relative energies given in bracket (in kcal · mol^{-1}) are calculated with B3LYP/6-31G//HF/6-31G levels

coordination involves the interaction of the cation with the carbonyl oxygen and morpholine substituent resulting a bridged structure (structures PM**1a**$_c$-bridged and PM**1a**$_b$-bridged). As the morpholine group can adopt a chair or boat like conformation, the combination of the site of coordination and the conformation of the morpholine group leads to six possible different structures of complex. The relative energy calculated at HF/6-31G and B3LYP/6-31G//HF/6-31G levels are presented (in Supplementary materials in Table S5). The results of the calculations clearly show that the bridged complexes, PM**1a**$_c$-bridged and PM**1a**$_b$-bridged are considerably more stable than all the other isomeric complexes in gas phase. For example, the predicted

DOI: 10.1002/poc

relative stability of PM**1a**-Li^+ complexes are found in the order: PM**1a**$_b$-bridged < PM**1a**$_c$-bridged < PM**1a**$_c$-O < PM**1a**$_b$-O < PM**1a**$_b$-O_{Mor} < PM**1a**$_c$-O_{Mor}.

The boat like conformation of the morpholine group leads to better interaction with cation since this conformation allows an interaction with both the oxygen and nitrogen. Therefore, the PM**1a**$_b$ isomer is almost 5 kcal/mol more stable than the corresponding PM**1a**$_c$ complex.

Analysis of the dipole moment of the optimised complexes in gas phase reveals strong variations of such properties as function of the site of complexation. For example, the PM**1a$_c$**-Mor complex exhibits very strong dipole moment (32.7 Debye) while PM**1a$_c$-**bridged has low polarity (4.2 Debye). It can be expected that PM**1a**$_c$-Mor could be more stabilised by solvent effect than PM**1a$_c$-**bridged complex. Therefore, calculations including the solvent effect with a continuum model (the explicit molecule of solvent has not been taken into account due to the prohibitive cost in time calculation) has been undertaken to estimate the solvent effect on the relative energy of the complexes. Consistent with our prediction, inclusion of solvent effect introduces relevant changes to the relative energy of the isomers. The most stable isomer in acetonitrile is the complex PM**1a$_c$**-Mor in which oxygen atom of morpholine group participates in formation of coordination bond (Table S5 in Supplementary materials).

The interaction of cation with TC isomer of PM**1b** can lead to the formation of three different structures. Indeed, the cation can coordinate only with crown-ether moiety (complex labelled as PM**1b**-C_w), with carbonyl atom oxygen (complex PM**1b**-O) or with both carbonyl atom and macrocylic moiety (complex PM**1b**-capped). The relative energies of these complexes are compiled (in Table S6 in Supplementary materials). It was shown that the PM**1b**-capped complex is the most stable minima in gas phase. Complex PM**1b**-O was found to be considerably less stable than those with participation of crown ether PM**1b**-C_w. A calculation was performed for PM**1b**-Li^+, PM**1b**-Na^+ and PM**1b**-Mg^{2+} complexes. In all cases PM**1b**-O structure is less stable by 33.0, 37.2 and 61.3 kcal/mol in comparison with PM**1b**-capped complex for Li^+, Na^+, Mg^{2+} respectively. It can also be noted the PM**1b**-O minima were not found with divalent Ba^{2+} and Pb^{2+} cations and the optimisation procedure converges toward capped complexes. The complexation of metal cation with macrocycle (structure PM**1b**-C_w) leads to less stable minimum in gas and solvent phases. However, divalent cations indicate strongest preference for capped structure (the PM**1b**-Cw complex is higher in energy than PM**1b-**capped complex by 30 kcal/mol) while the monovalent cation shows a less pronounced preference for PM**1b-**capped structure. For example, the PM**1b**-C_w complex obtained for Na^+ is less stable than PM**1b-**capped complex by only 5.7 and 0.4 kcal/mol in gas and condensed phases, respectively.

Coordination of cation with carbonyl oxygen atom in PM**1a**-O, PM**1b**-O, bridged and carbonyl-capped complexes leads to the pronounced variations of the conjugated pathway of the merocyanine. The shortening of the C2—C3, C4—C5 bond is accompanied by an increase of the C1—C2 and C3—C4 bond lengths. As a consequence of these geometric variations, the results (in Table S4 of Supplementary materials) indicate that bond-length alternation decreases upon cation complexation, that is, the contribution of the neutral VB structure becomes lower on moving from uncomplexed to complexed TC isomers.

Calculations show that the BLA index of PM**1b-**capped complexes continuously decreases in the series of cations from Li^+ to Pb^{2+}. This suggests that the increase in the charge of cation as well as its atomic radius leads to greater interaction with the crown ether and carbonyl group of merocyanine. One can notice that the calculated distance between cation and oxygen atoms in **1b**-capped structure reveals a stronger interaction with oxygen of carbonyl group than of crown ether oxygen. For example, the Pb^{2+}. . ..O-carbonyl distance is found 2.277 Å and the average Pb^{2+}. . ..O-crown ether distance is 2.803 Å. Analysis of Mulliken charge shows that this interaction is the result of charge transfer between cation and carbonyl oxygen atom: the net charge on carbonyl-oxygen atom is found -0.67 e and -0.52 e in **1b**-capped and **1b**-C_w, respectively. The calculated BLA for **1b**-C_w complexes do not show the same trend as for **1b**-capped and this index seems to depends only on the formal charge of the cation. The monovalent cation induces very weak changes in BLA when compared to uncomplexed structure (0.2 Å with Li+ and Na+) while the divalent cation leads to 0.15 Å value.

As the optical properties strongly depends on the geometry of the conjugated path,[18] it can be concluded from analysis based on BLA values that complex formation with mono-valent cation does not cause strong shift in the maximum absorption in PM**1b**-C_w and PM**1b-**capped structures while divalent-cation coordination induces strong bathochomic shift in PM**1b-**capped structure.

Binding energies of PM1b with cations. Accurate binding energy calcualtions is beyond the scope of this study. The binding energy of metal cation with 18-crown-6-ether was also calculated at the same level of calculations for comparison. It is interesting to note that the binding energies of PM**1b**-C_w TC complexes are consistently stronger than those for the complex with participation of crown ether moiety, adding 10 to 34 kcal/mol to the stability of the interaction (Table S7 in Supplementary materials). This result can originate in the strong N-donor property. Evidently, divalent cations exhibit strongest binding energy than in case of monovalent one and the magnitude of binding energy decreases on the radius of the cation increases. In the gas phase, the binding energies values were found to increase in the

DOI: 10.1002/poc

order: $Na^+ < Li^+ < Ba^{2+} < Pb^{2+} < Mg^{2+}$. This result is best understood by considering the fact that the hardness of the cation decreases as the radius increases. For PM**1b**-capped complexes, the binding energies values were calculated to 5 to 30 kcal · mol^{-1} lower than that calculated for PM**1b**-C_w. This suggests an additional interaction in PM**1b**-capped complex through charge transfer between the cation and the oxygen of the carbonyl group. Finally, on the basis of binding energy analysis, one can class the cation according to their affinity toward the crown-ether and susbstituted chromene in the following way: $Mg^{+2} > Pb^{+2} > Ba^{+2} > Li^+ > Na^+$.

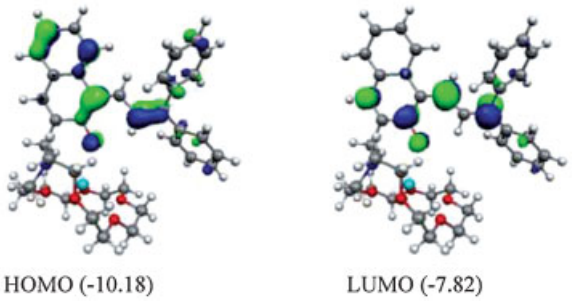

Figure 7. Plots and energies (eV) of HOMO and LUMO orbitals in the complex of TC isomer of **1b** with Ba^{2+} (capped geometry)

Theoretical electronic spectrum and molecular orbital analysis. The calculated maximum of the absorption long wavelength bands of the TC open merocyanine form of PM**1a** and PM**1b** and their 1:1 complex with Li^+, Na^+, Mg^{+2}, Ba^{+2} and Pb^{+2} cations (are listed in Table S10 of Supplementary materials).

The uncomplexed TC isomer of PM**1a** shows a strong absorption at 415 and 420 for the chair and twisted-boat conformation of morpholine group, respectively. Both values agree well with the experimental finding at 422 nm. The strong absorption for TC isomers of PM**1b**; that is PM**1b**-D_{3d}, PM**1b**-C_i, PM**1b**-C_{ii} and PM**1b**-C_{iii}; are ranging between 407 and 419 nm which match well with the experimental value (420 nm). The results indicate that the combination of HF/6-31G optimised geometry with B3LYP functional for TDDFT calculations is a methodology making it possible a high degree of accuracy in excitation energies with a reasonable computing time.

It is shown that complexation of carbonyl oxygen atom with Li^+ in PM**1a**-O and in bridged structures, PM**1a**-bridged, induces strong bathochromic shift. The maximum absorption is calculated at 461 nm and 478 nm for (PM**1a**$_c$-O)·Li^+ and (PM**1a**$_b$-bridged)·Li^+ complexes respectively. On the contrary, the complexation of oxygen of morpholine group does not lead to significant shift as compared to uncomplexed merocyanine. The maximum absorption bands for (PM**1a**$_c$-M)·Li^+ and (PM**1a**$_b$-M)·Li^+ are calculated at 439 and 452 nm respectively. The experimental data indicate no shift in the maximum absorption band when PM**1a** is irradiated in the presence of lithium or sodium cations. Thus, the results based on excitation energy calculations suggest that the complexation of the monovalent cation involves the morpholine group rather than the merocyanine part of the system. This hypothesis is consistent with the relative energies of the complexes found in solvent and discussed in previous section.

Coordination of the PM**1b** existing in the merocyanine form with cation leads to the bathochromic shift in the maximum absorption calculated as being a HOMO- → LUMO transition. These orbitals are mainly delocalised on the conjugated skeleton of the merocyanine form; see for example the HOMO and LUMO orbitals of capped complexe between 1b and Ba^{2+} displayed in Fig. 7. However, this shift strongly depends on the structure of the complex and the found order is PM**1b**-C_w < PM**1b**-capped < PM**1b**-O. For PM**1b**-C_w complex, the calculated lowest excitation energies are in a very good agreement with experimental data and only systematically underestimate is by 10 nm. According to the calculation the crown ether complexation by mono- or divalent cation in PM**1b**-Cw do not cause significant changes in the maximum absorption contrary to the experimental findings. On the other hand the coordination of the carbonyl oxygen in 1b-O complexes induces too strong bathochromic shift of the maximum absorption when compared to experimental data. Therefore both energetic and spectroscopic results suggest that the coordination of carbonyl oxygen atom by cation in 1b-O can be ruled out.

Coordination of the metal to the oxygen of the merocyanine form in the capped complexes induces a bathochromic shift by 12 nm, 15 nm and 31 nm for Mg^{2+}, Ba^{2+} and Pb^{2+} respectively. The maximum absorption are calculated at 455 nm, 450 nm, 495 nm, 498 nm and 515 nm with Na^+, Li^+, Mg^{2+}, Ba^{2+} and Pb^{2+} cations, respectively. These values are in good agreement with experimental data reported in Table 3. The bathochromic shift can be relied to the quinoidal deformation of the merocyanine type structure upon oxygen complexation which raise the HOMO energy orbital and lower the LUMO energy orbital. A relatively good correlation between HOMO-LUMO gap energies and the maximum absorption is obtained as shown in Fig. 8.

Liquid-liquid extraction properties of the benzochromenes 1b,c

The extraction capabilities of the azacrown ethers were tested in aqueous solution of various types of metal cations and counter ions and by using of different organic phases.

The extraction ability of azacrown ether ligands depends on the acidity of the solution. Thus, in the presence of

DOI: 10.1002/poc

Table 3. Calculated maximum absorption long wavelength of the TC isomers for PM**1a** and PM**1b** compounds

	λ_{max}			λ_{max}	
Complex PM**1a**	calclulated	Experi-mental	Complex PM **1b**	calclulated	Experi-mental
PM**1a**	—	422	PM **1b**	—	420
PM $\mathbf{1a}_c$	415	—	PM **1b**-D_{3d}	412	—
PM $\mathbf{1a}_b$	420	—	PM **1b**-C_i	414	—
PM **1a** · Li^+	—	420	PM **1b**-C_{ii}	419	—
(PM $\mathbf{1a}_c$-O) · Li^+	461	—	PM **1b**-C_{iii}	407	—
(PM $\mathbf{1a}_c$-M) · Li^+	439	—	PM **1b** · Li^+	—	450
(PM $\mathbf{1a}_c$-bridged) · Li^+	483	—	(PM1b-Cw) · Li^+	447	—
(PM $\mathbf{1a}_b$-O) · Li^+	461	—	(PM **1b**-O) · Li^+	471	—
(PM $\mathbf{1a}_b$-M) · Li^+	452	—	(PM **1b**-capped) · Li^+	455	—
(PM $\mathbf{1a}_b$-bridged) · Li^+	478	—	PM **1b** · Na^+	—	440
PM **1a** · Na^+	—	420	(PM **1b**-Cr) · Na^+	446	—
(PM $\mathbf{1a}_c$-O) · Na^+	443	—	(PM **1b**-O) · Na^+	457	—
(PM $\mathbf{1a}_c$-M) · Na^+	436	—	(PM **1b**-capped) · Na^+	450	—
(PM $\mathbf{1a}_c$-bridged) · Na^+	471	—	PM **1b** · Mg^{+2}	—	470
(PM $\mathbf{1a}_b$-O) · Na^+	440	—	(PM **1b**-Cr) · Mg^{+2}	484	—
(PM $\mathbf{1a}_b$-M) · Na^+	448	—	(PM **1b**-O) · Mg^{+2}	527	—
(PM $\mathbf{1a}_b$-bridged) · Li^+	466	—	(PM **1b**-capped) · Mg^{+2}	495	
PM **1a** · Mg^{+2}	—	460	PM **1b** · Ba^{+2}	—	460
(PM $\mathbf{1a}_c$-O) · Mg^{+2}	540	—	(PM **1b**-Cr) · Ba^{+2}	480	—
(PM $\mathbf{1a}_c$-bridged) · Mg^{+2}	438	—	(PM **1b**-capped) · Ba^{+2}	498	—
(PM $\mathbf{1a}_c$-M) · Mg^{+2}	543	—	PM**1b** · Pb^{+2}	—	500
(PM $\mathbf{1a}_b$-bridged) · Mg^{+2}	533	—	(**1b**-Cr) · Pb^{+2}	484	—
PM **1a** · Ba^{+2}	—	420	(PM **1b**-capped) · Pb^{+2}	515	
(PM $\mathbf{1a}_c$-O) · Ba^{+2}	602	—	—	—	—
(PM $\mathbf{1a}_c$-M) · Ba^{+2}	386	—	—	—	—
(PM $\mathbf{1a}_b$-bridged) · Ba^{+2}	546	—	—	—	—
PM **1a** · Pb^{+2}	—	465	—	—	—
(PM $\mathbf{1a}_c$-M) · Pb^{+2}	562	—	—	—	—
(PM $\mathbf{1a}_b$-bridged) · Pb^{+2}	547	—	—	—	—

protons the formation of protonated form of **1b,c** which is not able to bind metal cations was observed. The results indicate that the most effective extraction was found at pH 6.2 (Fig. S1 in Supplementary materilas shows the pH dependence of Ag^+ extraction). The following experiments were carried out at this condition.

In order to obtain the selectivity of ligand **1b,c** towards metal ion the extractability of metal salt Cs^+, Ag^+, Zn^{2+} and Eu^{3+} was carried out in the system metal salt-$NaClO_4$-MES/NaOH buffer 6.2/ligand-$CHCl_3$. The results were shown in Fig. 9a. As expected the ligands **1b,c** show very high extractability against the soft Ag^+. Whereas, Cs^+, Zn^{2+} and Eu^{3+} were not conveyed by this ligands into the organic phase. Ligands **1b,c** exhibit different Ag^+ extraction results according to the number nitrogen donor atoms in the crown ether fragment. The extraction of Ag^+ with the one nitrogen atom containing **1b** is among 4%. Whereas ligand **1c**, which provides two nitrogen atoms, extract of Ag^+ significant better with 90%.

Further, competitive Ag^+ extraction experiments with an equimolar addition of $Cu(ClO_4)_2$, $Hg(ClO_4)_2$ or

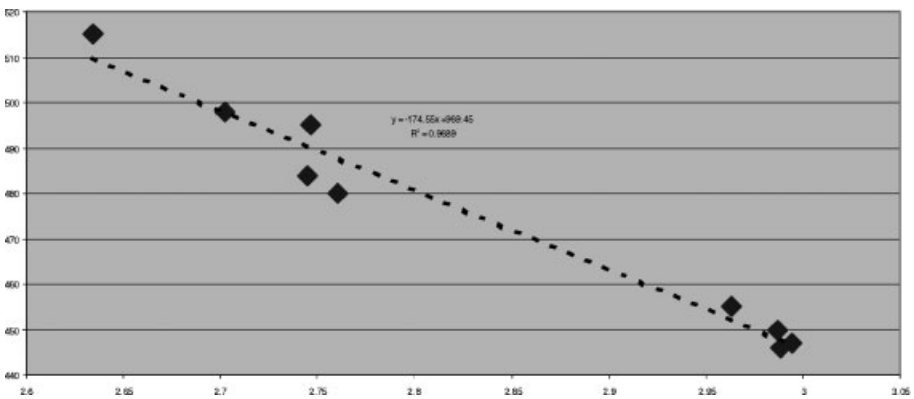

Figure 8. Correlation between the calculated maximum absorption (in nm) of TC isomer for **1b** and the HOMO-LUMO gap (in eV)

DOI: 10.1002/poc

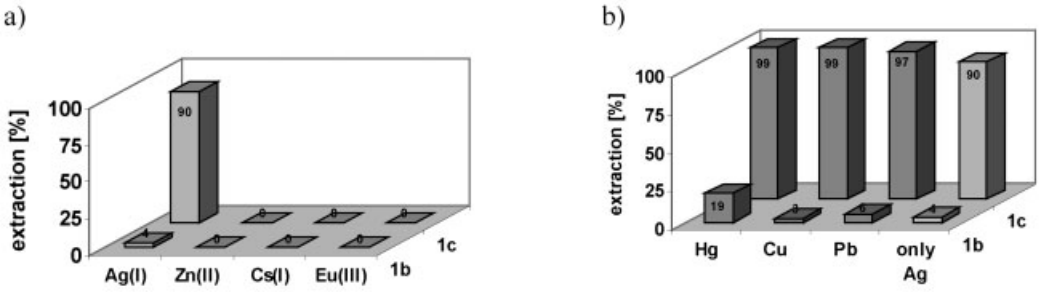

Figure 9. a) Extraction of Cs^+, Ag^+, Zn^{2+} and Eu^{3+}; b) extraction of Ag^+ in the presence of Pb^{2+}, Cu^{2+} and Hg^{2+}; $[M(ClO_4)_n] = 1{\cdot}10^{-4}$ M and $[NaClO_4] = 5{\cdot}10^{-3}$ M; [ligand] $= 1{\cdot}10^{-3}$ M in $CHCl_3$; MES/NaOH buffer pH = 6.2

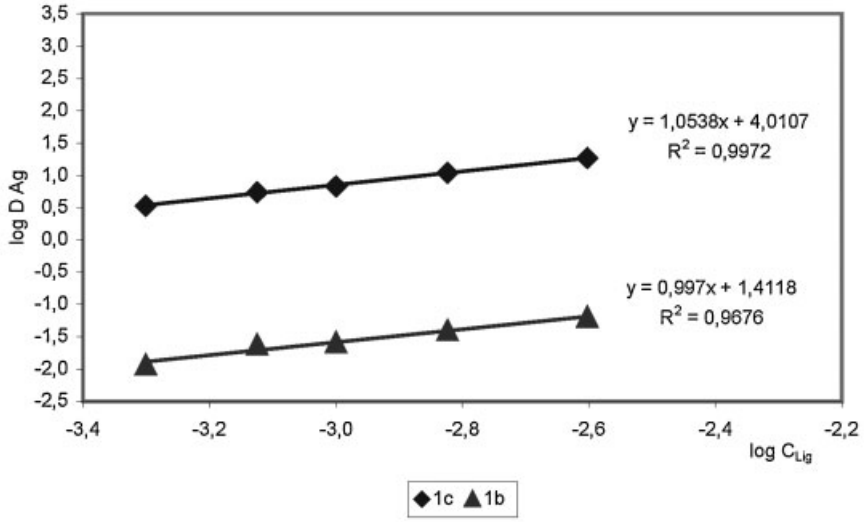

Figure 10. Extraction of Ag^+ with ligands **1b,c** depending on ligand concentration $[AgClO_4] = 1{\cdot}10^{-4}$ M, $[NaClO_4] = 5{\cdot}10^{-3}$ M; [ligand] $= 5{\cdot}10^{-4}$–$2.5{\cdot}10^{-3}$ M in $CHCl_3$; MES/NaOH buffer pH = 6.2

$Pb(ClO_4)_2$ were preformed, where the distribution of Ag^+ was monitored. As shown in Fig. 9b, the presence of the listed metal ions does not influence the results of the Ag^+ extraction. The results demonstrate the high selectivity toward Ag^+.

Details of the extracted metal complexes composition in the organic phase could be achieved by slope analysis of lg D_M–lg $c_{L(org)}$ diagram. Results of such experiments are shown for Ag^+ extraction with ligands **1b,c** in Fig. 10.

The straight line slopes for ligands **1b** and **1c** point out that the ligands form 1:1-complexes with Ag^+ under the chosen conditions.

The nature of anions influences on extraction is presented in Table 4. The ion, which passes into organic phase, must be firstly dehydrated in aqueous phase. Thereby lowly hydrated hydrophobic picrate anion is favoured, while highly hydrated, hydrophilic anion nitrate complicates the extraction. These is confirmed by the

Table 4. The extraction % of Ag^+ in presence of different counter ions $[AgClO_4] = 1{\cdot}10^{-4}$ M, $[AgNO_3] = 1{\cdot}10^{-4}$ M; $[NaClO_4] = 5{\cdot}10^{-3}$ M, $[NaNO_3] = 5{\cdot}10^{-3}$ M and [HPic] $= 5{\cdot}10^{-3}$ M respectively; [ligand] $= 1{\cdot}10^{-3}$ M in $CHCl_3$; and for different organic solvents, $[Ag^+] = 1{\cdot}10^{-4}$ M, [NaClO4] $= 5{\cdot}10^{-3}$ M; MES/NaOH-buffer pH = 6.2, [ligand] $= 1{\cdot}10^{-3}$ M, 25°C

	extraction % of AgX							
	In $CDCl_3$			$AgClO_4$				
Ligand	AgPic	$AgClO_4$	$AgNO_3$	$CHCl_3$	$C_6H_5NO_3$	$C_2H_4Cl_2$	$C_2H_4Cl_2$ (on sun light)	$C_2H_4Cl_2$ (irradiation at 254 nm)
1b	29	3.7	1	3.7	21.9	28.0	3.7	4.1
1c	83	90.2	18	90.2	99.4	99.3	90.2	90.6

DOI: 10.1002/poc

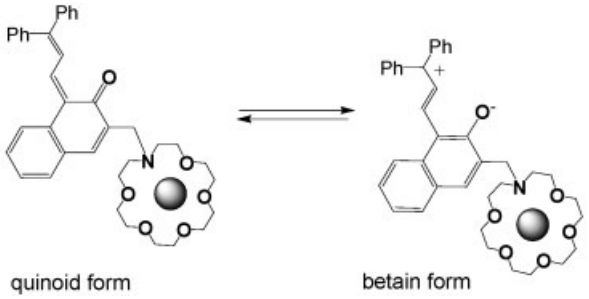

Scheme 9

obvious decrease of Ag^+ extraction from picrate to nitrate (see data in Table 4).

An important influencing factor on extraction equilibrium is the nature of employed solvent. Polar solvents usually lead to increase of the extraction, because the extracted ion pair is better stabilised in the more polar organic phase. In Table 4 it is shown, that extractability of Ag^+ with ligands **1b,c** in chloroform is clearly lower than in more polar solvents nitrobenzene and 1,2 dichlorethane.[25]

The influence of light on extraction of Ag^+ was analyzed (Table 4). The sun light or irradiation of the solution containing ligands slightly decreased the extraction ability of both ligands **1b,c**. In principal, the results are in agreement with the facts obtained by UV-spectroscopy and flash-photolysis method. Thus, Ag^+ forms the complex through the crown ether fragment. The open merocyanine form exists as mixture of quinoid and betain forms. The presence of positive charge in betain form prevents the introducing of metal cation into the molecule. It means that the transformation to the open form decreases the ability of photochromic ligand to bind the metal cations (Scheme 9).

CONCLUSIONS

Thus, the study demonstrates that the spectroscopic and kinetic behavior of the photomerocyanine isomers of the chromenes **1a-c** is strongly affected by complexation with metal cations. In the photomerocyanine form of compounds **1b,c** the formation of carbonyl-'capped' complexes with Ba^{2+} and Pb^{2+} was found.

We have explored the different site of coordination of mono- and divalent cations to determine the minimum-energy structure of PM**1a** and PM**1b** complexes in gas phase as well as in acetonitrile as solvent. With regard to the PM**1a** merocyanine isomer, the cation coordinates with both carbonyl oxygen and morpholine group in a bridged structure in gas phase, while most probably, the morpholine substituent is complexed by the cation in condensed medium. Concerning the PM**1b** merocyanine, the coordination of both carbonyl oxygen and crown-ether macrocyle with divalent cations in carbonyl-capped structure is found to be the most stable isomer in gas as well as in condensed media. The preference for capped structure with mono-valent cation such as Li^+ and Na^+ is less pronounced and the coordination of only crown-ether moiety by sodium cation can be even favoured in condensed medium.

The extraction of Ag^+ were found from aqueous solution to organic phase in present of benzochromene **1b,c**. The presence of two nitrogen atoms increases the extraction ability of the ligand. The extraction process was found to be of high selectivity. It is possible to extract Ag^+ from mixtures containing alkali, transition and heavy metal cations.

EXPERIMENTAL

Reagents and chemicals

The ligands **1a-c** were prepared as described in.[19,21]

Anhydrous MeCN, $LiClO_4$, $NaClO_4$, $CsClO_4$, $Mg(ClO_4)_2$, $Sr(ClO_4)_2$, $Ba(ClO_4)_2$, $AgClO_4$, $Cd(ClO_4)_2$, $Hg(ClO_4)_2$, $Cu(ClO_4)_2$, $Pb(ClO_4)_2$, $Zn(ClO_4)_2$ and $Eu(ClO_4)_3$ (Aldrich) were used as received.

X-ray diffraction analysis. Crystals of the compound suitable for X-ray crystallography were grown by slow evaporation from acetonitrile solutions. The structure was solved by direct methods and refined by full-matrix least-squares on F^2 in anisotropic approximation for all non-hydrogen atoms. The hydrogen atoms were calculated geometrically and refined using the 'riding' model.

The Bruker SAINT program[26] was used for data reduction. The SHELXTL-Plus[27] software was used for the structure solution and refinement. Crystallographic data and structure solution and refinement parameters are given in Table S3 (of Supplementary materials). Crystallographic data (excluding structure factors) for the structure have been deposited with the Cambridge Crystallographic Data Centre as supplementary publication no CCDC 245027. Copy of the data can be obtained free of charge on application to CCDC, 12 Union Road, Cambridge CB21EZ, UK (fax: (+44)1223-336-033; e-mail: deposit@ccdc.cam.ac.uk).

UV/Vis spectroscopy and kinetic measurements

UV/Vis absorption spectra were recorded with a spectrometer «USB2000» (kinetic measurements) and a spectrometer «Cary 50». The dark lifetimes of photomerocyanines of **1a-c** were measured using an experimental setup with a mercury flash lamp. The resolution time was less than 1 ms. The photostationary absorption spectra of merocyanine isomers were measured with the same setup upon steady-state irradiation of solutions with glass-filtered 365 nm light of a DRSh-250 high-pressure

DOI: 10.1002/poc

mercury lamp. The range of scanning was 400–750 nm with 1 nm increment.

Computational details

The compounds studied in this paper and its metal complexes present a significant computational challenge. At the heart of this challenge are the number of atoms (61 and 89 in cations complexes of **1a** and **1b**, respectively) and the structural flexibility of the crown ether macrocyclic backbone in **1b** compound. Restricted Hartree-Fock (RHF) wave functions were utilised to optimise molecular geometry in redundant internal coordinates. Geometry optimisations were carried out, without any symmetry constraint, using both the 6-31G basis set[28] and the SDD[29] pseudopotential for heavy atoms (Ba and Pb). Vibrational frequency calculations have been performed to ensure that the optimised structures (substituted benzochromene and complexes) correspond to energy minima. Solvents effects were included through single-point calculations using the polarised continuum model (PCM) of Tomasi and co-workers.[30] To investigate the binding affinities of **1b** for the cations, additional calculations were performed with density functional theory (DFT) were a wave function incorporating Becke's three-parameter hybrid functional (B3) was used along with the Lee-Yang-Parr correlation functional (LYP).[31] The binding affinities were evaluated by computing the energies of the gas-phase association reactions:

$$\mathbf{M}^{+} + \mathbf{1b} \rightarrow \mathbf{M}^{+}/\mathbf{1b}$$

where the free substituted **1b** benzochromene corresponds to the lowest-energy conformation isomer. Basis set superposition error was accounted by the full counterpoise correction of Boys and Bernardi.[32] Single point calculations of each species of the previous equation were performed at DFT level of calculations using the HF/6-31G optimised geometry. Both small 6-31G and more extended 6-31+G(d) basis set were used for such calculations. The low lying excited states were calculated within the adiabatic approximation of time dependent density[33] with the B3LYP hybrid functional. It is known that the B3LYP functional overestimate the electron delocalisation,[34] therefore the HF/6-31G optimised molecular geometry were used as input geometry for TDDFT calculations. Vertical excitation energies were computed for the first 10 singlet excited states, in order to reproduce the UV–visible spectra of free and complex compounds. All the calculations have been performed using Gaussian 98 program package.[35]

Liquid-liquid extraction using radiotracer technique

The liquid-liquid extraction experiments were performed at $24 \pm 1^{\circ}$C in microcentrifuge tubes ($2\,cm^3$) by means of mechanical overhead shaking. The phase ratio $V_{(org)}$: $V_{(w)}$ (500 μl each) was 1:1. In the water phase the initial concentration of the metal ion was $1 \cdot 10^{-4}$M I counter ion was added in a concentration of $5 \cdot 10^{-3}$M as there sodium salt ($NaNO_3$; $NaClO_4$) and acid form (Hpic), respectively . The Ligand concentration in the organic phase was $1 \cdot 10^{-3}$M The shaking time was chosen as 30 min. All experiments were preformed at a pH of 6.2 by using the MES/NaOH buffer system (MES – 2(N-Morpholine)ethansulfonic acid). After the extraction, all samples were centrifuged and the phases separated. The distribution of the metal ion concentration was detected in both phases radio metrically by γ-radiation of ^{110m}Ag, ^{137}Cs, ^{65}Zn and ^{153}Eu in a NaI (TI) scintillation counter (Cobra II/Canberra-Packard). The equilibrium pH was measured by using an InLab micro pH electrode.

The easily accessible experimental parameter in liquid-liquid extraction systems represents the distribution ratio D_M, the quotient of the metal concentrations in the organic and aqueous phase, or the per centage extractability (E%): $D_M = C_{M(org)}/C_{M(w)}$; $E[\%] = 100 \cdot D_M/(D_M+1)$

Acknowledgements

This work was supported by the Russian Foundation for Basic Research (Projects 05-03-33268, 03-03-32888) and the program ARCUS.

REFERENCES

1. Brown GH (ed.). *Photochromism*, Wiley-Interscience: New York, 1971.
2. McArdle CB (ed.). *Applied Photochromic Polymer Systems*, Blackie: New York, 1992.
3. Dürr H, Bouas-Laurent H (eds). *Photochromism: Molecules and Systems*, Elsevier: Amsterdam, 1990.
4. Becker RS, Michl J. *J. Am. Chem. Soc.* 1966; **88**: 5931–5933.
5. Crano JC, Flood T, Knowles D, Kumar A, Van Gemert B. *Pure Appl. Chem.* 1996; **68**: 1395–1398.
6. Gabbutt CD, Heron BM, Instone AC, Horton PN, Hursthouse MB. *Tetrahedron* 2005; **61**: 463–471.
7. Coelho PJ, Salvador MA, Oliveira MM, Carvalho LM. *J. Photochem. Photobiol. A: Chem.* 2005; **172**: 300–307.
8. Frigoli M, Mehl GH. *Chem. Comm.* 2004; 2040–2041.
9. Inouye M, Ueno M, Tsuchiya K, Nakayama N, Konishi T, Kitao T. *J. Org. Chem.* 1992; **57**: 5377–5383.
10. Minkin VI. *Chem. Rev.* 2004; **104**: 2751–2776.
11. Kimura K, Yamashita T, Yokoyama M. *J. Chem. Soc., Perkin Trans. 2* 1992; 613–619.
12. Tanaka M, Kamada K, Ando H, Kitagaki T, Shibuyani Ya, Kimura K. *J. Org. Chem.* 2000; **6**: 4342–4347.
13. Nakamura M, Fujioka T, Sakamoto H, Kimura K. *New J. Chem.* 2002; **26**: 554–559.
14. Kimura K, Sakamoto H, Nakamura M. *Bull. Chem. Soc. Jpn.* 2003; **76**: 225–245.
15. Alfimov MV, Fedorova OA, Gromov SP. *J. Photochem. Photobiol. A:Chem.* 2003; **158**: 183–198.
16. Fedorova OA, Ushakov EN, Fedorov YV, Strokach YP, Gromov SP. Macrocyclic systems with photoswitchable functions. In *Macrocyclic Chemistry: Current Trends and Future Perspectives*, Gloe K (ed.). Springer: Dordrecht, Berlin, 2005; 235–252.

DOI: 10.1002/poc

17. Stauffer MT, Knowles DB, Brennan C, Funderburk L, Lin FT, Weber SG. *Chem. Comm.* 1997; 287.
18. Fedorova OA, Maurel F, Ushakov EN, Nazarov VB, Gromov SP, Chebun'kova AV, Feofanov AV, Alaverdian IS, Alfimov MV, Barigelletti F. *New J. Chem.* 2003; **27**: 1155–1167.
19. Ahmed SA, Tanaka M, Ando H, Iwamoto H, Kimura K. *Eur. J. Org. Chem.* 2003; 2437–2442.
20. (a) Habata Y, Akabori S. *Coord. Chem. Rev.* 1996; **148**: 97–126; (b) Heidari N, Thaler A, Schneider H, Cox GB. *Inorg. Chem. Acta* 1998; **279**: 186–191.
21. Chebun'kova AV, Strokach YuP, Valova TM, Fedorova OA, Gromov SP, Alfimov MV, Lokshin V, Samat A. *Mol. Cryst. Liq. Cryst.* 2005; **430**: 67–73.
22. Ushakov EN, Gromov SP, Buevich AV, Baskin II, Fedorova OA, Alfimov MV, Eliasson B, Edlund U. *J. Chem. Soc., Perkin Trans. 2* 1999; 601–607.
23. Fedorova OA, Gromov SP, Pershina YV, Sergeev SS, Strokach YP, Barachevsky VA, Alfimov MV, Pèpe G, Samat A, Guglielmetti R. *J. Chem. Soc., Perkin Trans. 2* 2000; 563–571.
24. Delbaere S, Luccioni-Houze B, Bochu C, Teral Y, Campredon M, Vermeersch G. *J. Chem. Soc., Perkin Trans. 2* 1998; 1153–1158.
25. Richardt C. *Solvents and Solvent Effects in Organic Chemistry*, 2nd Edition, VCH: Weinheim, 1990.
26. *SAINT*, Version 6.02A, Bruker AXS, Inc., Madison, Wisconsin (USA), 2001.
27. *SHELXTL-Plus, Release 5.10*, Bruker AXS, Inc., Madison, Wisconsin (USA), 1997.
28. Frisch MJ, Trucks GW, Schlegel HB, Scuseria GE, Robb MA, Cheeseman JR, Zakrzewski VG, Montgomery JA, Stratmann RE, Burant JC, Dapprich S, Millam JM, Daniels AD, Kudin KN, Strain MC, Farkas O, Tomasi J, Barone V, Cossi M, Cammi R, Mennucci B, Pomelli C, Adamo C, Clifford S, Ochterski J, Petersson GA, Ayala PY, Cui Q, Morokuma K, Malick DK, Rabuck AD, Raghavachari K, Foresman JB, Cioslowski J, Ortiz JV, Stefanov BB, Liu G, Liashenko A, Piskorz P, Komaromi I, Gomperts R, Martin RL, Fox DJ, Keith T, Al-Laham MA, Peng CY, Nanayakkara A, Gonzalez C, Challacombe M, Gill PMW, Johnson BG, Chen W, Wong MW, Andres JL, Head-Gordon M, Replogle ES, Pople JA. *Gaussian 98* (Revision A.1), Gaussian, Inc., Pittsburgh, PA, 1998.
29. Ditchfield R, Hehre WJ, Pople JA. *J. Chem. Phys.* 1971; **54**: 724–728.
30. (a) Fuentealba P, Preuss H, Stoll H, Szentpaly LV. *Chem. Phys. Lett.* 1989; **89**: 418–422; (b) Fuentealba P, Szentpaly LV, Preuss H, Stoll H. *J. Phys. B* 1985; **18**: 1287–1296; (c) Wedig U, Dolg M, Stoll H, Preuss H. In *Quantum Chemistry: The Challenge of Transition Metals and Coordination Chemistry*, Veillard A (ed.). Reidel: Dordrecht 1986; 79; (d) Kaupp M, Schleyer PV, Stoll H, Preuss H. *J. Chem. Phys.* 1991; **94**: 1360–1366.
31. Cossi M, Scalmani G, Rega N, Barone V. *J. Chem. Phys.* 2002; **117**: 43–54.
32. Becke AD. *J. Chem. Phys.* 1993; **98**: 5648–5652; Lee C, Yang W, Parr RG, *Phys. Rev. B* 1988; **37**: 785–789.
33. Boys SF, Bernardi F. *Mol. Phys.* 1970; **19**: 553–566.
34. Bauernschmitt R, Ahlrichs R. *Chem. Phys Lett.* 1996; **256**: 454–464.
35. (a) Wannere CS, Sattelmeyer KW, Schaefer HF, Schleyer PR. *Angew. Chem. Int. Ed.* 2004; **43**: 4200–4212; (b) Wannere CS, Sattelmeyer KW, Schaefer HF, Schleyer PR. *J. Am. Chem. Soc.* 1999; **121**: 10788–10793; (c) Geskin VM, Dkhissi A, Brédas JL. *Int. J. Quantum Chem.* 2003; **91**: 350–354.

DOI: 10.1002/poc